

LEO V: A COMPANION OF A COMPANION OF THE MILKY WAY GALAXY?

V. BELOKUROV¹, M. G. WALKER¹, N. W. EVANS¹, D. C. FARIA¹, G. GILMORE¹, M. J. IRWIN¹, S. KOPOSOV², M. MATEO³,
 E. OLSZEWSKI⁴, D. B. ZUCKER¹

SUBMITTED TO *Astrophysical Journal Letters*

ABSTRACT

We report the discovery of a new Milky Way satellite in the constellation Leo, identified in data from the Sloan Digital Sky Survey. It lies at a distance of ~ 180 kpc, and is separated by $\lesssim 3^\circ$ from another recent discovery, Leo IV. We present follow-up imaging from the Isaac Newton Telescope and spectroscopy from the Hectochelle fiber spectrograph at the Multiple Mirror Telescope. Leo V's heliocentric velocity is $\sim 173.3 \pm 3.1$ kms⁻¹, offset by ~ 40 kms⁻¹ from that of Leo IV. A simple interpretation of the kinematic data is that both objects may lie on the same stream, though the implied orbit is only modestly eccentric ($e \sim 0.2$)

Subject headings: galaxies: dwarf — galaxies: individual (Leo) — Local Group

1. INTRODUCTION

In the last few years, there have been numerous discoveries of ultra-faint Milky Way satellites, primarily because the Sloan Digital Sky Survey (SDSS) allows the detection of galaxies with central surface brightnesses as faint as 30 mag arcsec⁻². The new discoveries include 10 new Milky Way dwarf galaxies, together with 4 unusually extended or faint globular clusters (Willman et al. 2005; Zucker et al. 2006a,b; Belokurov et al. 2006, 2007; Irwin et al. 2007; Walsh et al. 2007; Koposov et al. 2007). The purpose of this *Letter* is to announce the discovery of an additional Milky Way satellite, probably a dwarf galaxy that may be undergoing disruption, at a heliocentric distance of ~ 180 kpc in the constellation of Leo. Following the convention for naming dwarf spheroidals, we call it Leo V. It lies very close to one of our other recent discoveries, namely Leo IV (Belokurov et al. 2007). Hence, it is a companion to a companion of the Milky Way Galaxy.

2. DATA AND DISCOVERY

SDSS imaging data are produced in five photometric bands, namely u , g , r , i , and z (see e.g., Adelman-McCarthy et al. 2006; Gunn et al. 2006). The data are automatically processed through pipelines to measure photometric and astrometric properties (Lupton, Gunn, & Szalay 1999; Smith et al. 2002; Ivezić et al. 2004) and de-reddened using Schlegel et al. (1998). Data Release 6 (DR6) covers ~ 8000 square degrees, primarily around the North Galactic Pole.

Koposov et al. (2008) argued that almost all the satellites in SDSS DR5 had been found and that any further candidates would require substantial followup imaging to confirm their nature. Accordingly, we pursued the strategy of acquiring deeper imaging of possible candidates of lower statistical significance than 6 (see eq (7) of Koposov et al. (2008)). This is of course rather inefficient, and generally yields negative results. As the significance is lowered, there are many candidates that are selected, due to Poisson noise and false positives induced by large-scale structure. Additional reasons are thus needed to warrant the expenditure of time and effort. In the case of Leo V, its actual significance is ~ 4 , but the presence of possible blue horizontal branch (BHB) stars in the SDSS data was such an indicator.

Fig. 1 shows the SDSS view of Leo V. As usual with the ultrafaint dwarfs, no object is visible in the SDSS cut-out. The next two panels of Fig. 1 show the density of resolved stars and galaxies, respectively. There is a visible overdensity in stars at the location of Leo V, but the background shows extensive substructure, leaving the nature of any object unclear. There is also an overdensity of galaxies close to the location of Leo V. Fine-tuning the selection of stars from the color-magnitude diagram (CMD) to likely members, however, does yield a convincing object, as shown in the upper right panel of Fig. 1. The lower panels show three CMDs. The first is restricted to stars within 2' of the center of Leo V, and shows a tentative red giant branch (RGB) and a handful of horizontal branch stars. On moving outwards to stars within 5', the horizontal branch swells and the red clump becomes visible. The comparison CMD shown in the lower middle right panel is composed of stars within

TABLE 1
 PROPERTIES OF THE LEO V SATELLITE

Parameter ^a	
Coordinates (J2000)	11 31 09.6 +02 13 12.0
Coordinates (Galactic)	$\ell = 261.86^\circ, b = 58.54^\circ$
r_h (Plummer)	0.8 ± 0.1
$\mu_{0,V}$ (Plummer)	27.5 ± 0.5^a
$(m-M)_0$	$21^m 25$
$M_{tot,V}$	$-4^m 3 \pm 0.5$
v_\odot	$+173.3 \pm 3.1$ kms ⁻¹
v_{GSR}	$+60.8$ kms ⁻¹

^a Surface brightnesses and integrated magnitudes are corrected for the mean Galactic foreground reddening, $A_V = 0.1$.

¹ Institute of Astronomy, University of Cambridge, Madingley Road, Cambridge CB3 0HA, UK; vasilij,walker,nwe@ast.cam.ac.uk

² Max Planck Institute for Astronomy, Königstuhl 17, 69117 Heidelberg, Germany

³ Department of Astronomy, University of Michigan, Ann Arbor, MI 48109, USA

⁴ Steward Observatory, University of Arizona, Tucson, AZ 85721, USA

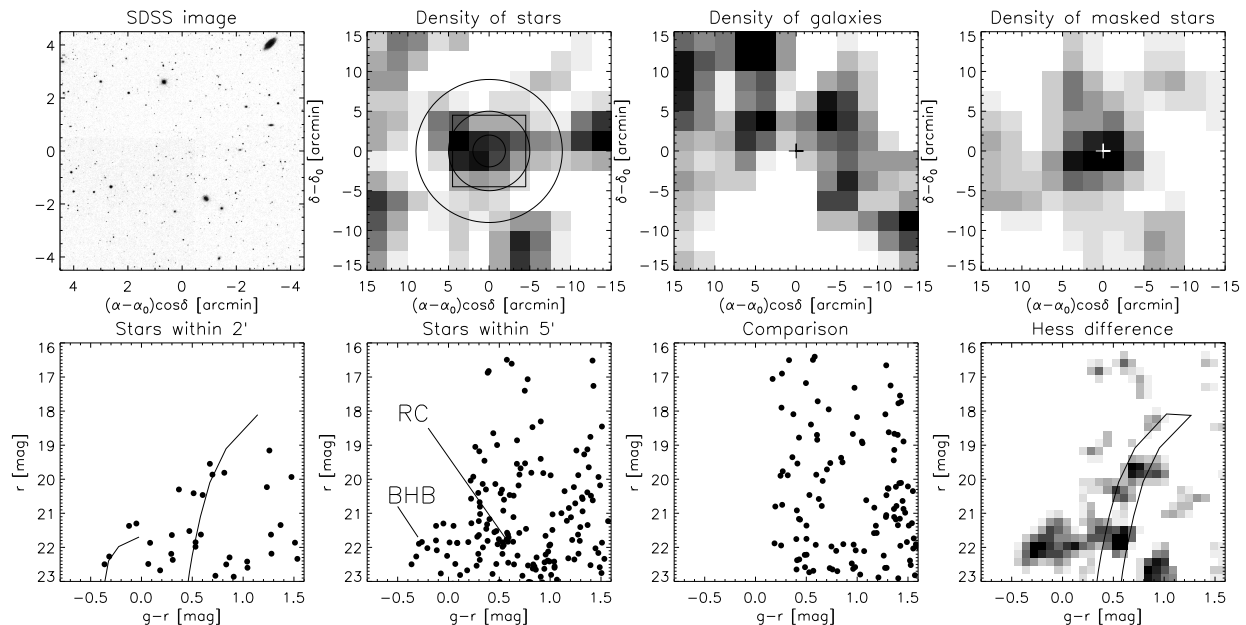


FIG. 1.— The Leo V Satellite: *Upper Left*: SDSS cut-out ($9' \times 9'$) around the center of Leo V. *Upper Middle Left*: The spatial distribution of all objects classified as stars in a $30' \times 30'$ field. *Upper Middle Right*: The spatial distribution of all objects classified as galaxies. *Upper Right*: Density of candidate RGB stars selected with the CMD mask shown in the panel directly below. *Lower Left*: CMD of all stars in a circle of radius $2'$, which is expected to be dominated by Leo V members. *Lower Middle Left*: CMD of all stars within $5'$, with the red clump and BHB marked. *Lower Middle Right*: CMD of stars within the annulus $9'$ to $10.3'$ showing the foreground. *Lower Right*: Difference in Hess Diagrams, showing the red giant branch and BHB of Leo V. The mask is built with M92 ridgelines offset to the distance modulus of 21.25.

an annulus of $9'$ to $10.3'$ and shows the foreground. In the differential Hess diagram in the lower right panel, there is a convincing detection of the red giant and horizontal branch. The mask is based on the ridgeline of M92 ($[\text{Fe}/\text{H}] = -2.28$, Clem 2005) and is used to select possible RGB members.

Fig. 2 is a gray-scale density plot of the BHB stars selected with the cuts: $20.5 < r < 22.5$, $-0.6 < g - r < 0$ and $0.5 < u - g < 1.5$, based on the cuts of Sirko et al. (2004). Leo IV and Leo V are clearly visible and separated by only $\sim 2.8^\circ$ on the sky. There are other overdensities of BHB candidates, but most are correlated with galaxy clusters as shown in the bottom panel.

3. PHOTOMETRIC AND SPECTROSCOPIC FOLLOW-UP

Follow-up observations of Leo V were made on 7/8 March 2008 (UT) using the 2.5 m INT telescope and the WFC mosaic camera, with four $2\text{k} \times 4\text{k}$ pixel EEV CCDs, a field of view of roughly $30' \times 30'$, and a scale of $0.33'' \text{ pixel}^{-1}$ at the field center. Leo V was observed with total integrations of 1800s in g and r filters, split into $3 \times 600\text{s}$ with $\sim 10''$ shifts in-between each exposure. The typical seeing measured directly from the images was rather poor, varying between $\sim 1.7 - 2.0''$. Data were reduced using a general purpose pipeline for processing wide-field optical CCD data (Irwin & Lewis 2001). Images were de-biased, trimmed, cross-talk corrected, and then flatfielded and gain-corrected to a common internal system using clipped median stacks of nightly twilight flats. For each image frame, an object catalog was generated and used to update the world coordinate system prior to stacking each set of 3 frames. A final set of object catalogs were generated from the stacked images and

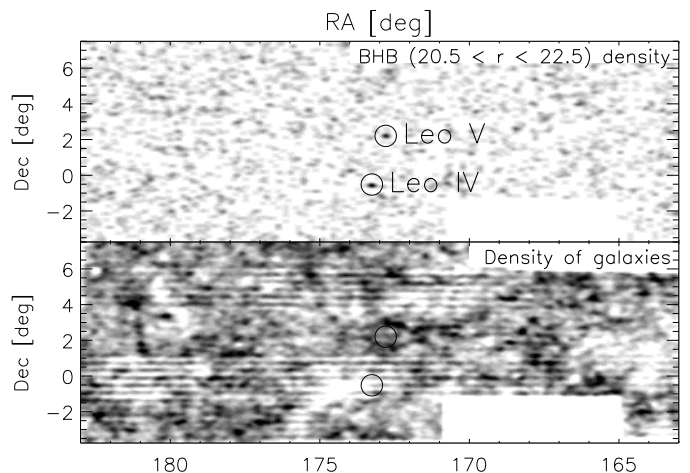


FIG. 2.— *Top*: Density of BHB candidate stars in $5'$ square pixels, smoothed with a $10'$ FWHM filter. Leo IV and Leo V are marked by circles. *Bottom*: Large scale structure at the same location. Note that there is correlation between overdensities in the two panels due to object misclassification.

objects were morphologically classified as stellar or non-stellar (or noise-like). The detected objects in each pass-band were then merged by positional coincidence (within $1''$) to form a combined g, r catalog and photometrically calibrated on the SDSS system using stars in common.

With the poorer than average seeing, the INT data are only about 0.5 magnitude deeper than the SDSS data. Fig. 3 shows the CMDs of stars within $3'$ and $6'$ from the center. There is some improvement in the tightness of the red giant branch and especially the horizontal

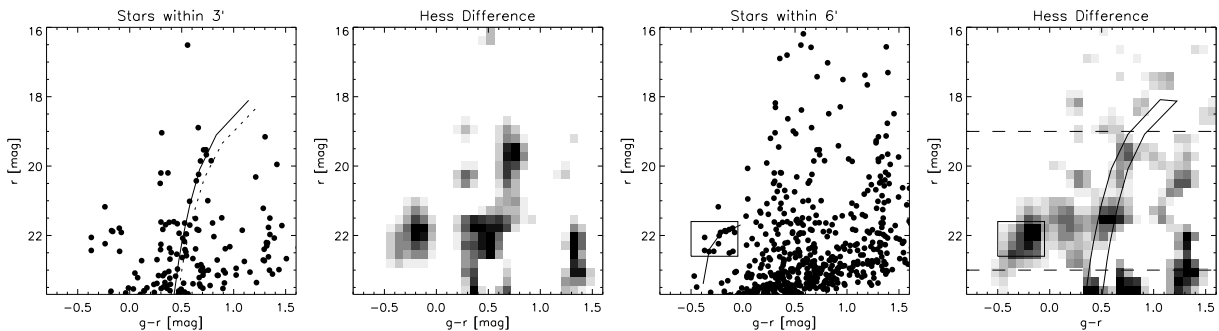


FIG. 3.— Leo V in INT data: *Left and middle left*: CMD and Hess differential diagram of stars within $3'$ with ridgelines of M92 (solid) and M13 (dotted). Note the possible detection of a red horizontal branch. *Middle right and right*: The same but for stars within $6'$. Note that the BHB stars sit tightly on the ridgeline of M92s BHB, offset to the distance modulus of Leo V. The masks are used to select red giants (within the magnitude range marked by the dashed lines) and BHBs.

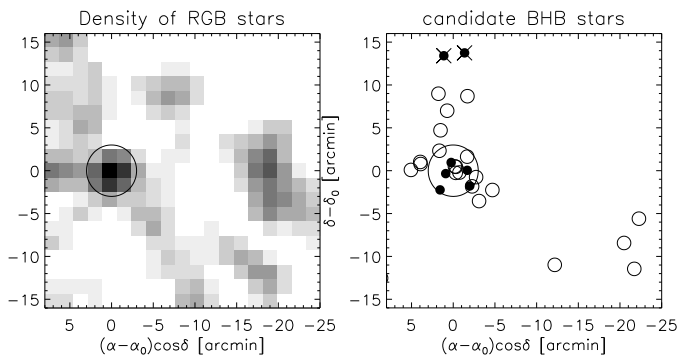


FIG. 4.— *Left*: The density of RGB candidate members selected from the INT photometry. The extent of Leo V as judged from two half-light radii is marked. *Right*: The locations of BHB candidate members. Note that the BHB distribution is elongated and more extended than that of the RGB stars. Black dots are RGB stars with spectroscopy, $v_{\odot} \approx 173 \text{ km s}^{-1}$ and low ΣMg (see Fig. 5).

branch. The BHBs are now aligned with the ridgeline derived from M92, which is used to measure the distance to Leo V as $180 \pm 10 \text{ kpc}$. Having fixed the distance, we can experiment with different stellar populations, shown in the first panel by the ridgelines of M92 (solid) and M13 (dotted). M13 ($[\text{Fe}/\text{H}] = -1.54$) has a giant branch that is too red, while the more metal-poor M92 ($[\text{Fe}/\text{H}] = -2.28$) is a closer match to the stellar population. We also show masks wrapped around the red giant and horizontal branches which are used to select the candidate members for Fig. 4. The two populations are distributed differently; most of the light from the RGB stars is limited to the inner $3'$, whereas the BHB stars extend out to at least $10'$. This phenomenon has been seen in other dSphs such as Carina and Sculptor (Harbeck et al. 2001; Tolstoy et al. 2004; Koch et al. 2006)

The number density of stars defined by the RGB and BHB selection boxes is sharply peaked in the central region with a half-light radius, from Plummer and exponential model fits, of $\sim 0.8'$, or 42 pc for a distance of 180 kpc . However, the profile also shows an extended plume of stars slightly above the general background level (Fig. 4). This extended appearance makes the luminosity of the satellite difficult to estimate directly. We first converted the number density radial profile to a (luminosity-weighted) surface brightness profile to directly estimate

the central surface brightness. Integrating the Plummer law model fit then gives a total flux from resolved stars. Comparison with the M92 luminosity function suggests we are missing roughly $1/2$ of the light from fainter members which would yield a total magnitude in the central $3'$ radius region of $M_{\text{tot},V} \approx -4^{\text{m}}3$. This number is a lower limit on the luminosity, as it ignores any contribution at larger radius, such as from the plume.

We obtained spectra of 159 red giant candidates using the Hectochelle fiber spectrograph at the MMT 6.5-m telescope on Mt. Hopkins, Arizona. Spectroscopic targets were selected from the red giant branch of Leo V (Figure 5) within a field of radius $30'$, centered on the object. The Hectochelle spectra sample at high resolution ($R \sim 25000$) the wavelength range $5150 - 5300 \text{ \AA}$, which includes the prominent magnesium triplet (MgT) absorption feature. For each of two distinct Hectochelle configurations targeting Leo V, we obtained $3 \times 2700\text{s}$ exposures during the nights of 28 and 29 May 2008. Spectra were reduced following a procedure described by Mateo et al. (2008). For each star we measure the (solar rest frame) line-of-sight velocity, v_{\odot} , by cross-correlating the spectrum against a high-S/N template of known velocity. We also measure the pseudo-equivalent width of the MgT feature, ΣMg , using the technique of Walker et al. (2007). The data include 70 stars with INT photometry, of which 52 lie inside the mask shown in the left panel of Fig. 5. We calculate errors in v_{\odot} and ΣMg from models which consider the quality of the cross-correlation function and spectral S/N, respectively (see Mateo et al. 2008; Walker et al. 2007).

The left panel of Figure 5 shows the CMD of the INT stars with the candidate selection mask superimposed. This is slightly broader than the one shown in the right-most panel of Fig. 3, to include all possible candidates. Solid dots show stars with spectra, gray lie outside the mask and black lie inside. We circle the five most probable Leo V members, which have a mean velocity of $173.3 \pm 3.1 \text{ km s}^{-1}$. The remaining three panels show the correlation between r magnitude, distance from center and ΣMg . Note in particular that in the plane of $(v_{\odot}, \Sigma\text{Mg})$, the giants in Leo V are clearly separated from the dwarfs in the thick disk and halo of the Milky Way. It is also clear that there are 2 more possible members that lie at large distance from the center.

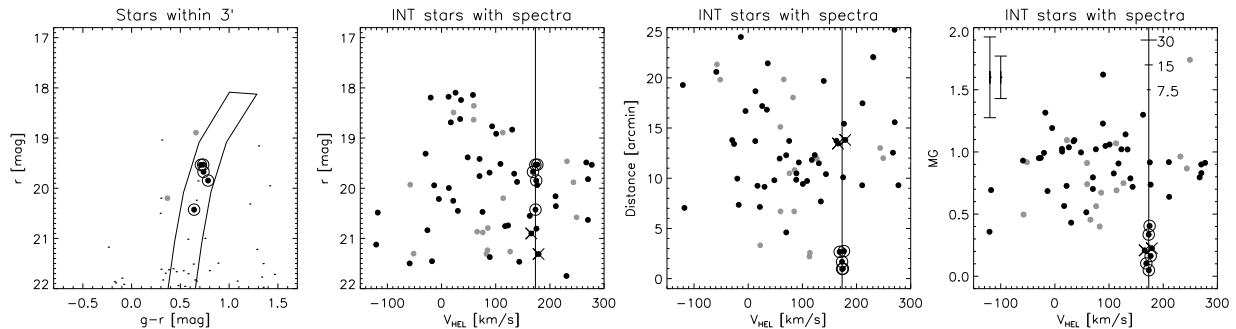


FIG. 5.— *Left*: CMD of INT stars within $3'$, shown as small dots, together with the mask selecting most likely RGB members. Stars with spectra are full dots, with gray used for stars outside the mask and black for those within. The five most probable members are circled. *Middle left*: r magnitude versus velocity for all INT stars with spectra. The line marks is the likely systemic velocity of Leo V (173.3 km s^{-1}). *Middle right*: Distance from the center as a function of velocity. *Right*: The pseudo-equivalent width ΣMg as a function of velocity. The mean and median error in ΣMg is shown as vertical bars in the left-hand corner. Note the clear separation of the giants in Leo V from Galactic stars. There are two more likely members (marked with crosses) located in the data cluster. The three horizontal bars have widths corresponding to 7.5 , 15 and 30 km s^{-1} to aid calibration.

4. DISCUSSION AND CONCLUSIONS

Leo V is most probably a new dwarf galaxy, based on the presence of an old, metal-poor population with a characteristic size of between 50 and 200 pc. There are several hints that it may be a disrupting satellite, but our data do not support the idea that it is merely an overdensity in a stellar stream. The most remarkable feature of Leo V is the disparity in the spatial extent of the RGB and BHB populations. The red giants are confined to a tight core of ~ 50 pc, whereas the BHBs extend out at least as far as 200 pc. There even appear to be BHBs associated with Leo V at distances of 500 pc. One possible explanation for the apparent difference is that the RGB stars do follow the BHBs much further out, perhaps because the object is disintegrating, but they are more difficult to distinguish from the foreground populations in our data. A hint that this the case is perhaps provided by the two RGB candidates that are even further than the most distant BHBs, although their membership needs to be confirmed. With deeper photometry reaching down to the turn-off, it should be possible to verify this hypothesis. Another explanation is that the RGB and BHB populations probe different epochs of star formation in an ultra-low mass system.

Leo V's possible association with Leo IV is also unique. Although there are other examples of dSphs separated on the sky by a few degrees – such as CVn I and CVn II – they are at different distances and velocities. By contrast, Leo IV is at a heliocentric distance of ~ 160 kpc (Belokurov et al. 2007) and a heliocentric velocity of 132 km s^{-1} (Simon & Geha 2007). These are very close to our estimates of ~ 180 kpc and 173 km s^{-1} for the distance and velocity of Leo V. Referred to the Galactic Standard of Rest, the velocities of Leo IV and V are low, 11.0 km s^{-1} and 59.5 km s^{-1} respectively. Using the velocity distribution for the $\rho \sim r^{-3.5}$ radial profiles given

in Evans et al. (1997) to construct artificial samples of 50 satellites, we estimate that there is a $\lesssim 1$ per cent probability of this coincidence happening by chance. We remark that one of BHB stars considered by Simon & Geha (2007) for possible membership of Leo IV, but then discarded, has a heliocentric velocity of 160 km s^{-1} . This hints at the possible existence of extended stellar structures around Leo IV and Leo V. If Leo IV and Leo V are assumed to be on the same stream, then the orbit can be computed, assuming a singular isothermal sphere with amplitude $v_0 = 220 \text{ km s}^{-1}$. The pericenter is ~ 160 kpc and the apocenter is ~ 244 , so that the eccentricity is modest ($e = 0.2$) and the orbit never approaches the inner parts of the Milky Way (in which case both objects should be relatively intact, at odds with their seemingly irregular appearances).

Leo V may prove to be an important object for testing theories of galaxy formation. Ricotti et al. (2008) has argued that very old dwarf galaxies must form preferentially in chain structures, tracing the filamentary dark matter in the early universe. These chains or groups of dwarfs may retain some of their integrity even on accretion and merging into the Milky Way halo. Is it possible that Leo IV and Leo V are two links in such a chain?

Funding for the SDSS and SDSS-II has been provided by the Alfred P. Sloan Foundation, the Participating Institutions, the National Science Foundation, the U.S. Department of Energy, the National Aeronautics and Space Administration, the Japanese Monbukagakusho, the Max Planck Society, and the Higher Education Funding Council for England. The SDSS Web Site is <http://www.sdss.org/>. EO acknowledges NSF grants AST-0205790, 0505711, and 0807498; MM acknowledges NSF grants AST-0206081 0507453, and 0808043

REFERENCES

- Adelman-McCarthy, J. K., et al. 2006, ApJS, 162, 38
 Belokurov, V. et al. 2006, ApJ, 647, L111
 Belokurov, V. et al. 2007, ApJ, 654, 897
 Clem, J. L. 2005, PhD Thesis, University of Victoria
 Evans, N. W., Hafner, R. M., & de Zeeuw, P. T. 1997, MNRAS, 286, 315
 Gunn, J.E. et al. 2006, ApJ, in press
 Harbeck, D., et al. 2001, AJ, 122, 3092
 Irwin, M. J., et al. 2007, ApJ, 656, L13
 Irwin, M.J., & Lewis, J. 2001, New Astronomy Review, 45, 105
 Ivezić, Ž. et al., AN, 2004, 325, 583

- Koch, A., Grebel, E. K., Wyse, R. F. G., Kleyna, J. T.,
Wilkinson, M. I., Harbeck, D. R., Gilmore, G. F., & Evans,
N. W. 2006, *AJ*, 131, 895
- Koposov, S., et al. 2007, *ApJ*, 669, 337
- Koposov, S., et al. 2008, *ApJ*, in press, arXiv:0706.2687
- Li, Y.-S., & Helmi, A. 2008, *MNRAS*, 385, 1365
- Lupton, R., Gunn, J., & Szalay, A. 1999, *AJ*, 118, 1406
- Mateo, M., Olszewski, E. W., & Walker, M. G. 2008, *ApJ*, 675,
201
- Ricotti, M., Gnedin, N. Y., & Shull, J. M. 2008, *ArXiv e-prints*,
802, arXiv:0802.2715
- Schlegel, D. J., Finkbeiner, D. P., & Davis, M. 1998, *ApJ*, 500,
525
- Simon, J. D., & Geha, M. 2007, *ApJ*, 670, 313
- Sirko, E., et al. 2004, *AJ*, 127, 899
- Smith, J. A., et al. 2002, *AJ*, 123, 2121
- Tolstoy, E., et al. 2004, *ApJ*, 617, L119
- Walker, M. G., Mateo, M., Olszewski, E. W., Bernstein, R., Sen,
B., & Woodroffe, M. 2007, *ApJS*, 171, 389
- Willman, B., et al. 2005, *ApJ*, 626, L85
- Walsh, S. M., Jerjen, H., & Willman, B. 2007, *ApJ*, 662, L83
- Zucker, D. B., et al. 2006a, *ApJ*, 643, L103
- Zucker, D. B., et al. 2006b, *ApJ*, 650, L41